2008 American Control Conference
Westin Seattle Hotel, Seattle, Washington, USA
June 11-13, 2008

Smooth trajectories for imaging string-like samples in AFM: A preliminary study

Peter I. Chang and Sean B. Andersson
Aerospace and Mechanical Engineering
Boston University, Boston, MA 02215
{itchang,sanderss}@bu.edu

Abstract— **In this paper, we present a high-level feedback control algorithm for rapid imaging in atomic force microscopy (AFM). This algorithm is designed for samples which are string-like, such as DNA and biopolymers. The tip control of the microscope is performed in real-time while probing the unknown sample based on feedback from the tip and a model of the sample. This model is continually updated based on the measurements. To avoid exciting unwanted dynamics in the AFM system, the tip is steered at a constant velocity along a sinusoidal trajectory whose average is the estimate of the sample curve. We discuss the advantages of the algorithm and some of the challenges which must be overcome to make this technique a viable approach to AFM imaging.**

I. Introduction

In this paper we present a method for the rapid imaging of string-like structures using an atomic force microscope. Data being measured by the tip of the microscope are used in real-time to estimate parameters of the model of the sample curve. This estimated model is then used to steer the tip such that it remains in the vicinity of the sample. As a result the overall imaging time is greatly reduced by reducing the total area that needs to be imaged. This work builds upon earlier efforts of one of the authors and proposes a smooth trajectory for the tip to avoid exciting unwanted dynamics in the actuators.

Atomic force microscopy (AFM) is one of the most versatile tools for studying systems with nanometer-scale features. It is particularly interesting to controls engineers in that its operation depends entirely on a feedback loop [1]. Images are built pixel-by-pixel through a raster-scan and typically take on the order of a few seconds to minutes to acquire. In recent years, the technology has been used with increasing prevalence to study dynamic phenomena in systems with nanometer-scale features. The standard approach is time-lapse imaging in which a sequence of images is acquired and then processed to extract information about the motion. While the method has been used successfully to study a variety of phenomena in molecular biology (e.g. [2], [3]) and materials science (e.g. [4], [5]), the achievable time-scale is far slower than that of many important phenomena. This severely restricts the applicability of the approach.

Researchers are pursuing several techniques to improve the temporal resolution of AFM. These include tuning the components of the microscope to improve performance [6], novel mechanism designs [7], [8] and actuation schemes [9], and the use of modern control theory to increase the scanning speed while maintaining image quality [10]–[12]. For recent reviews of the control issues and approaches, see [13], [14].

Our approach is both novel and complementary to other high-speed AFM techniques. Our general methodology is to take advantage of *a priori* knowledge about the sample of interest to develop feedback control laws which replace the raster scan with a more efficient sampling scheme. Non-raster methods can be found in a wide variety of engineering disciplines where a short-range or point sensor is used to collect data [15]. In prior work we introduced a string scanning technique in which the tip was steered along short line segments transverse to the string-like sample. Using the Frenet-Serret framework for the spatial evolution of a curve, the evolution of the curve was predicted based on current measurements.The resulting control law kept the tip in the vicinity of the sample, greatly reducing the time to acquire the image [16]. However, the short line segments require rapid acceleration of the tip since it must be brought to a full stop at the end of every segment. This can excite unwanted higher modes of the actuators and the tip-sample system, leading to errors in the tip trajectory, lower-quality images, and severe limitations on the imaging speed.

In this work we propose a smooth tip trajectory to replace the short line segments. The tip is moved at constant velocity along a sinusoidally varying curve. The spatial frequency of this curve determines the spatial resolution of the resulting image of the sample. To ensure that the tip tracks the sample, the mean of the tip trajectory is set to be the estimated curve representing the sample. This estimate is continually updated in real-time based on data measured by the microscope. The rest of this paper is organized as follows. In the next section we detail the tip trajectory. The algorithm to estimate the curve representing the sample is presented in Section III while the advantages of the approach and challenges that need to be overcome are described in Section IV.

II. A trajectory for smooth scanning

We are interested in samples which are well-modeled as planar curves. Examples include a variety of biological poymers such as actin, DNA, and microtubules, as well as materials such as carbon nanotubes and nanowires. Typically the curve would represent the centerline of the sample but it may be used to represent the boundary of a sample as well. The spatial evolution of a curve in the plane can be described using the Frenet-Serret frame [17]. Under this model, the

curve is given by

$$\frac{dx_d(s)}{ds} = q_1(s), \tag{1a}$$

$$\frac{dq_1(s)}{ds} = \kappa(s)q_2(s), \tag{1b}$$

$$\frac{dq_2(s)}{ds} = -\kappa(s)q_1(s). \tag{1c}$$

Here $x_d(s)$ is the position vector with respect to a fixed frame to the point on the curve at arclength s, $q_1(s)$ is the tangent vector at s, $q_2(s)$ the normal vector at that point, and $\kappa(s)$ is the curvature. As discussed in Section IV, the rate of change of the curvature is assumed to be slow relative to the spatial sampling rate defined by the imaging scheme given by (2) below.

Motivated by the goal of reducing the time to image the sample, we want to avoid wasting time acquiring data unrelated to the sample. To achieve this, we propose to steer the tip along a trajectory which remains in the vicinity of curve. One such curve is given by

$$x_{\text{tip}}(s) = x_d(s) + A\sin(\omega s)q_2(s). \tag{2}$$

Here A is a parameter defining the amplitude of the scanning and ω is the spatial frequency of oscillation. The parameter A is analogous to the length of a single scan line under the standard raster-scan approach while ω determines the spatial resolution of the resulting image. The curve x_d is the desired average trajectory, namely the underlying sample curve, and s is the arclength parameter of that curve. As discussed in Section III, this curve can be estimated using only recent measurements of the tip. In Figure (1) we illustrate the trajectory defined by (2) for a circular path.

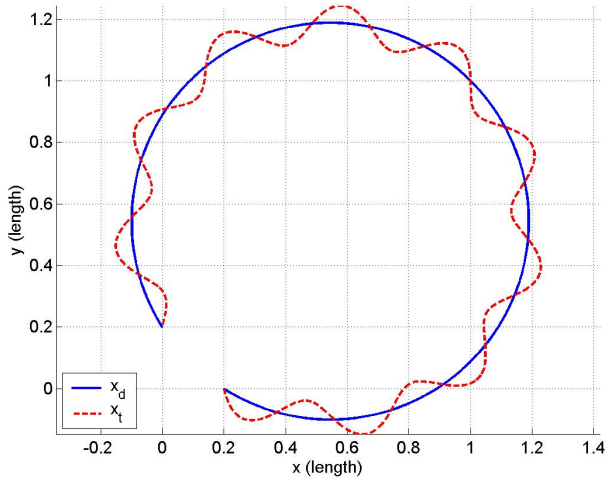

Fig. 1. Example of the tip trajectory along a circular path. The trajectory is defined by (2) where $x_d(s)$ is the circle. The parameters were set to $A = 0.2$ units and ω = 10 radians/unit.

In order to steer the tip in an actual instrument, this trajectory must be defined in terms of time, not as a function of the arclength of the (unknown) sample curve,

$$x_{\text{tip}}(t) = x_d(s(t)) + A\sin(\omega s)q_2(s(t)). \tag{3}$$

We must therefore determine the relationship between the arclength parameter and time.

In order to avoid exciting unwanted dynamics in the actuators and the tip-sample system, it is important to keep the motion of the tip of microscope as smooth as possible. To achieve this, we choose a constant speed for the tip, $v_{\text{tip}} = \|\dot{x}_{\text{tip}}\|$ where $\|\cdot\|$ is the standard Euclidean norm. From (2), the time derivative of tip position is

$$\dot{x}_{tip}(t) = \left(\frac{dx_d(s(t))}{ds} + A\omega\cos(\omega s(t))q_2(s(t)) + A\sin(\omega s(t))\frac{dq_2(s(t))}{ds}\right)\dot{s}. \tag{4}$$

where $\dot{}$ indicates the derivative with respect to time. Using the relationship from (1), and taking the Euclidean norm of (4), the speed of the tip in terms of s and t is given by

$$v_{\text{tip}} = \dot{s}\sqrt{(1 - A\kappa\sin(\omega s))^2 + A^2\omega^2\cos^2(\omega s)}. \tag{5}$$

Define $f(s)$ by

$$f(s) = \sqrt{(1 - A\kappa\sin(\omega s))^2 + A^2\omega^2\cos^2(\omega s)}.$$

Integrating (5) under the assumption that the velocity is constant, we find

$$v_{\text{tip}}t = \int_0^s f(\sigma)\,d\sigma \tag{6}$$

Since the curvature is assumed to be slowly-varying, we may take it to be constant over small ranges of s and, by extension, t. We must then consider two cases, $\kappa = 0$ and $\kappa \neq 0$. When the curvature is zero, that is, when the underlying path x_d is a straight line, $f(s)$ reduces to $\sqrt{1 + A^2\omega^2\cos^2(\omega s)}$. Solving (6) yields the relationship between time and arclength to be

$$t = \frac{\sqrt{1 + A^2\omega^2}}{v_{\text{tip}}\omega}E(\omega s, \frac{A\omega}{\sqrt{1 + A^2\omega^2}}). \tag{7}$$

where E is the incomplete elliptic integral of the second kind defined as

$$E(\phi, k) = \int_0^\phi \sqrt{1 - k^2\sin^2(x)}\,dx.$$

When $\kappa \neq 0$, the solution for x_{tip} must be obtained by integrating (6).

In order to use this approach to steer the tip, the current arclength must be determined from the current value of t by inverting the relationship given by (6). In Figure 2, we show two examples of the resulting relationship between time and arclength, one for the case of zero curvature and one for the case of nonzero curvature. In this example, the scan amplitude A was set to 2 units, the scan frequency ω was set to 4 rads/unit, and the tip speed was set to 1 unit/sec. The inversion can be done off line and the results stored in a look-up table.

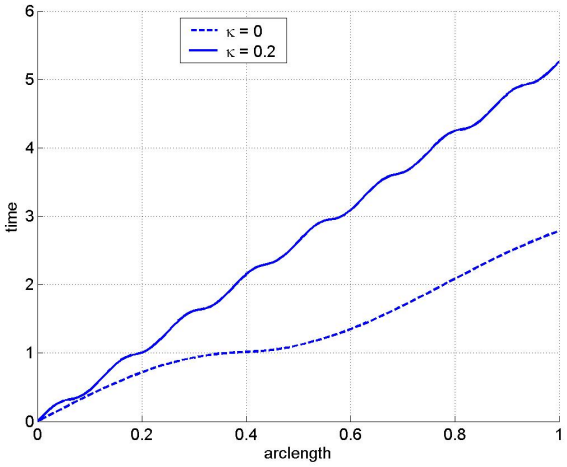

Fig. 2. Relationship between arclength s and time t for $\kappa = 0$ and $\kappa = 0.2$. To implement the desired tip trajectory defined by (3), the arclength s must be determined given the current time by inverting this relationship.

III. Estimating the Sample Path

The path $x_d(\cdot)$ of the sample is of course not known *a priori*. However, using the equations for the spatial evolution of the curve as given by (1), this path can be estimated at least locally if the current position state and the curvature are known. Assuming that the curvature is slowly changing with respect to the spatial frequency defined by ω, we may take the curvature to be constant between two subsequent crossings of the sample by the tip (see Figure 1). We can then propagate the estimate of the sample curve using the current state and curvature according to the Frenet-Serret frame model and thereby steer the tip according to (2). Upon the next intersection with the sample, the state of the model and the curvature are updated and the process is continued.

The model is updated after every crossing of the tip trajectory and the sample curve. In what follows, we introduce a subscript k to indicate the instance of the kth such crossing. In between crossings the curvature estimate, κ is assumed to be constant while the position x_d, tangent q_1, and normal q_2 are evolved according to the Frenet-Serret frame model.

The estimation process described below has been discussed previously in [16], [18] and thus only an overview is given here.

A. Estimating the state x_d, q_1, and q_2

The position x_d is updated according to the measured point of intersection with the sample. This measurement can be obtained from the height data of the tip under contact mode imaging, from the amplitude data under AC mode imaging, or from any signal dependent on the tip-sample interaction. One approach involving a maximum likelihood estimator to compensate for noisy measurements is described in [16]. An alternative approach for rapid detection of this intersection based on the innovations process of a Kalman filter is described in [19].

To estimate the current tangent and normal vectors, we introduce a heading direction θ with respect to the global frame, and relate this to the Frenet-Serret frame according to

$$q_1 = \begin{pmatrix} \cos(\theta) \\ \sin(\theta) \end{pmatrix}, \quad q_2 = \begin{pmatrix} -\sin(\theta) \\ \cos(\theta) \end{pmatrix}.$$

The current value of θ is determined using the last two scanned measurement points from a simple Euler approximation

$$\theta_k = \tan^{-1}\left(\frac{[x_{mk-2}]_2 - [x_{mk-1}]_2}{[x_{mk-2}]_1 - [x_{mk-1}]_1}\right). \tag{8}$$

Here x_m denotes the measured (scanned) points. While it is certainly possible to develop more accurate estimators, it is reasonable to assume that the step size along the sample will be small enough such that this first-order approach is sufficiently accurate.

The curvature κ is estimated using Heron's formula [20]. Let A, B, C be three successive and nearby points on a curve and let a, b, c denote the Euclidean distances between the points (see Figure 3). The radius of curvature of the circle is given by

$$\kappa(A, B, C) = \pm 4\frac{\sqrt{l(l-a)(l-b)(l-c)}}{abc} \tag{9}$$

where $l = \frac{1}{2}(a+b+c)$ is the semi-perimeter of the triangle. The estimate of the curvature of the string at the point x_{mk} is given by (9) where the points A, B, C correspond to x_{mk-2}, x_{mk-1}, and x_{mk}. The sign is taken to be positive if the cosine of the angle between the vector connecting the points x_{mk-1} and x_{mk} and the normal vector is positive (so that the normal vector points "inside" the curve.

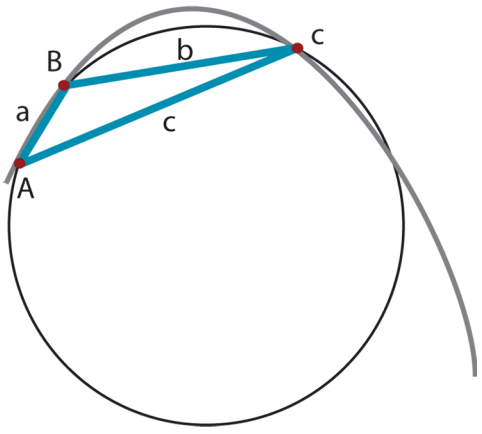

Fig. 3. The curvature is estimated by using Heron's formula for the circle defined by the three most recent measured points on the curve.

Noise in the measurement of the height and lateral position of the tip propagate through these estimators. Furthermore because the heading direction is estimating a derivative and the curvature a second-order derivative, any such noise is amplified. Noise may also be introduced through numerical error when inverting the relationship between time and

arclength. As discussed in [16], the effect of these noise processes can be mitigated through the use of a Kalman filter on the estimators.

B. Scan initialization

To initialize the scan, a standard raster-scan approach is performed until an intersection with a sample curve is detected. To determine the initial heading direction, the tip is scanned along a circle centered at this intersection point until the curve is intersected again. With these first two points the heading direction can be estimated according to (8) and the algorithm begun under the assumption of zero curvature. So long as the spatial frequency of the tip trajectory is high relative to the true curvature, the tip will once again cross the sample. With three points the true curvature can be estimated according to (9).

C. Algorithm summary

Algorithm 3.1: Curve tracking with smooth tip trajectory

0. *Initialize:* A raster scan is performed to find the start of the underlying curve followed by a circular search to determine the initial heading direction θ. The initial curvature is set to 0.
1. *Update tip trajectory:* Steer the tip according to (3) until another intersection is detected.
2. *Estimate parameters:* Determine x_{mk} from the point of intersection, estimate θ_k and κ_k according to (8) and (9) and filter.
3. $k \to k+1$ and go to 1.

Although not explicitly considered here, we note that the parameters A and ω can be modified according to the model estimate. For example, the spatial frequency can be made small in regions of small curvature to move the tip rapidly along relatively uninteresting segments of the sample and large in regions of high curvature to increase the spatial resolution in particularly interesting regions. The amplitude A may be set larger if the knowledge of the curve evolution is less certain, thereby giving a larger "search" range to ensure intersection or made very small to decrease to path length of the tip trajectory, thereby reducing the overall imaging time. Further issues related to these scan parameters is discussed in the following section.

An example trajectory resulting from this algorithm is shown in Figure (4). In this simulation the underlying curve (drawn in blue) is not know *a priori* but is estimated as described above. On the figure, the tip trajectory is dotted in black while the red circles highlights the intersection points. All length scales are normalized to a reference unit. The figure indicates the effect of varying the parameters A and ω.

IV. Discussion

The goal of this work is to develop algorithms for the rapid imaging of string-like samples through non-raster approaches. In this section we discuss some of the challenges which will need to be overcome as the work progresses from the initial concept presented here to a useful imaging tool.

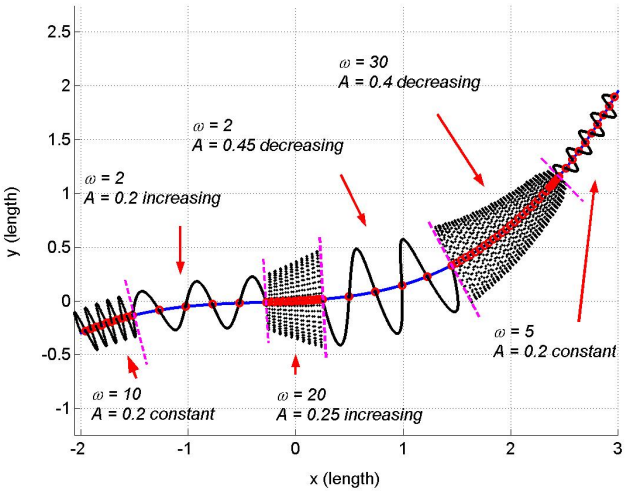

Fig. 4. Example result of the scanning algorithm. In this image the unknown true curve x_d is indicated in blue and the tip trajectory in black. The points of intersection are shown in red. Based on these intersections, the state of the curve model and the curvature are estimated and then updated according to the Frenet-Serret frame equations. The tip trajectory shown has different regions which illustrate the effect of varying the scan parameters ω and A.

When images are generated from a raster scan, the underlying sample grid has evenly spaced samples. This makes interpretation of the surfaces generated from the scans straightforward. However data acquired from non-raster methods are not uniformly spaced. As a result there is a need to interpolate the data to produce an image. While a variety of techniques exist, including triangularization and Kriging, there is no universally accepted or all-purpose tool. More research is needed to understand how to create accurate images from noisy, non-raster data. For further comments, see [15].

Both the nonlinear interaction of the tip and the sample as well as the measurement noise will have a large impact on this imaging technique. Due to the nonlinear characteristics of the tip-sample system, the estimate of the location of the sample when the tip moves across the sample curve in one direction will not exactly match the estimate as the tip moves across the sample in the opposite direction. This will give rise to a small but periodic "dither" in the estimates. Similarly, measurement noise will cause errors in this estimate. These errors will propagate through to the estimates of the heading direction and curvature. So long as these errors are small, it can be expected that the stable nature of the system will allow the underlying curve to be tracked. However, they will give rise to relatively large shifts in the normal direction q_2. Because this direction directly influences the tip trajectory, the commanded path of the tip will become more complex. This is illustrated in Figure 5. In this image, a small error in the estimation of the intersection is introduced, giving rise to interesting variations in the sinusoidal trajectory. While these effects can be mitigated somewhat through appropriate filtering, especially the contribution coming from

measurement noise, it is to be expected that a thorough understanding of these issues will aid in designing schemes to reduce their influence.

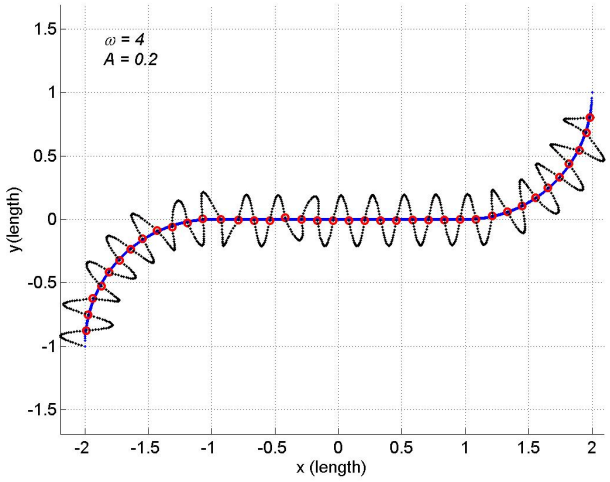

Fig. 5. Effect of estimation error on the scan trajectory. Due to noise and nonlinear tip-sample interactions, the estimated position of the intersection of tip trajectory and the sample curve will have some error. Because the heading direction and curvature are determined from a sequence of these positions, the error will propagate and be amplified through the estimates of these parameters and will thus have a direct effect on the tip trajectory. As shown here, a small error in the estimate gives rise to a "wobble" of the tip trajectory. Despite this wobble, a fairly uniform sampling of the curve is achieved.

As discussed above, the choice of ω defines the spatial resolution of the scan while the choice of A defines the spatial extent of the scan. However, these parameters cannot be selected completely independently of the underlying curvature or the rate of change of curvature. There are two possible errors which can arise from a mismatch between the sample and the parameters. In the first, a large or rapidly varying curvature may bend the curve in such a way that the tip crosses the sample farther along than the distance defined by ω. This is illustrated in Figure 6. In this case, a "jump" along the sample occurs and a region of the sample will not be imaged at all. While it may be possible to detect such an event, perhaps by monitoring the phase of the sinusoid at which the intersection occurs, in general the system will be unaware that such a jump occurred and thus the generated image will be false. This event can be prevented by adapting the amplitude and spatial frequency to the curvature of the sample. How such an adaptation would be performed remains an open question.

The second possibility is that the sample curve can bend away from the tip trajectory fast enough so that no intersection occurs. In this case the sample will be lost entirely, as illustrated in Figure 7. Once again, proper choice of the amplitude and spatial frequency can prevent this event.

Finally, the trajectories produced by the algorithm introduced here are quite different from the standard raster-scan pattern. As a result, one must consider the capabilities of the actuation system to steer the tip along these paths. One of the

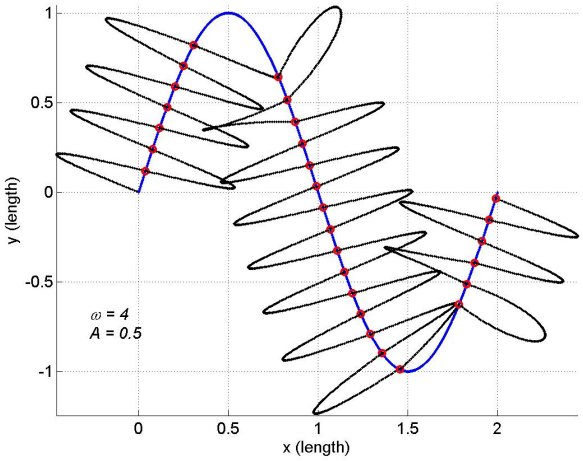

Fig. 6. Large curvatures or rapid changes in curvature can give rise to undesired intersections. As shown in the figure, if the amplitude of the scan is too large with respect to the curvature and rate of change of curvature, the tip trajectory may intersect the sample at an undesired position, leading to a skip of a section of the sample.

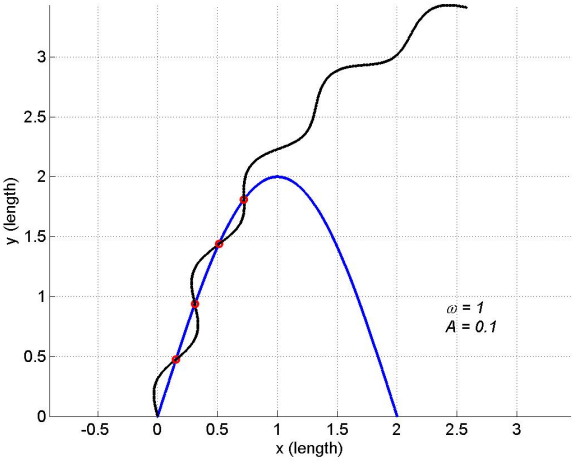

Fig. 7. Large curvatures or rapid changes in curvature can lead to a miss of the sample. If the spatial frequency (and amplitude) are too small with respect to the curvature or rate of change of curvature, it is possible that the tip trajectory will not intersect the sample at all. Under this event imaging will be halted.

most common actuators is the three-degree-of-freedom piezo tube as developed by Binnig and Smith [21]. Because such a scanner has similar mechanical properties in the two lateral directions, it is particularly well-suited for the trajectories generated by the approach discussed in this paper. However, the lateral directions are not commonly provided with sensors and are therefore controlled in an open-loop mode. However, with the arbitrary trajectories necessary for the non-raster approach, a feedback control approach is essential to mitigate the effect of measurement noise on the path estimation.

An alternative approach is the use of a separate x-y scanner based on a frame-within-a-frame design. This scheme minimizes physical coupling between the different directions and

typically includes sensing on the lateral position. However, the stage is often asymmetric. With the standard raster-scan approach, this asymmetry can be taken advantage of by using the lower-mass axis as the fast-scan direction. Under the non-raster approach, the overall system would be limited in speed by the slower of the two axes.

Advanced control schemes motivated by the need for high-speed AFM will likely also be useful when developing controllers for accurate tracking of the desired tip trajectory. An overview and discussion of these approaches can be find in [13]. While still in the research phase, new designs of actuation systems for high-speed AFM are symmetric and include accurate sensing on the lateral position [8]. Such systems may be particularly relevant to non-raster methods. For further discussion of actuation schemes in AFM, see [1].

V. Conclusions

In this paper we have proposed an algorithm for the rapid of imaging of string-like samples using atomic force microscopes. The approach builds upon prior work of one of the authors and introduces a smooth trajectory for the microscope tip. Such a trajectory will allow the tip to be moved at a constant speed throughout the imaging process, avoiding the excitation of unwanted dynamics in the actuators. This will allow the tip to be moved at higher speeds while maintaining tracking accuracy along the desired path. We have outlined several challenges that need to be overcome in order that this approach can be a viable method for fast imaging in AFM. Our ongoing work is addressing these issues.

Acknowledgements

This work was supported in part by NSF grant DBI-0649823.

References

[1] D.Y. Abramovitch, S. B. Andersson, L. Y. Pao, and G. Schitter, "A tutorial on the mechanisms, dynamics and control of atomic force microscopes," in *Proceedings of the American Control Conference*, 2007, pp. 3488–3502.

[2] A. P. Gunning, A. R. Kirby, A. R. Mackie, P. Kroon, G. Williamson, and V. J. Morris, "Watching molecular processes with the atomic force microscope: dynamics of polymer adsorption and desorption at the single molecule level," *Journal of Microscopy*, vol. 216, no. 1, pp. 42–56, October 2004.

[3] H. Janovjak, A. Kedrov, D. A. Cisneros, K. T. Sapra, J. Struckmeier, and D. J. Müller, "Imaging and detecting molecular interactions of single transmembrane proteins," *Neurobiology of Aging*, vol. 27, no. 4, pp. 546–561, April 2006.

[4] J. Hahm and S. J. Sibener, "Time-resolved atomic force microscopy imaging studies of asymmetric PS-b-PMMA ultrathin films: Dislocation and disclinationi transformations, defect mobility, and evolution of nanoscale morphology," *Journal of Chemical Physics*, vol. 114, no. 10, pp. 4730–4740, March 2001.

[5] J. K. Hobbs, C. Vasilev, and A. D. L. Humprhis, "Real time observation of crystallization in polyethylene oxide with video rate atomic force microscopy," *Polymer*, vol. 46, no. 23, pp. 10 226–10 236, November 2005.

[6] T. Ando, N. Kodera, E. Takai, D. Maruyama, K. Saito, and A. Toda, "A high-speed atomic force microscope for studying biological macromolecules," *Proceedings of the National Academy of Sciences of the United States of America*, vol. 98, no. 22, pp. 12 468–12 472, December 2001.

[7] G. Schitter, K. J. Åström, B. DeMartini, G. F. Fantner, K. Turner, P. J. Thurner, and P. K. Hansma, "Design and modeling of a high-speed scanner for atomic force microscopy," in *Proceedings of the American Control Conference*, 2006, pp. 502–507.

[8] G. Schitter, "Advanced mechanical design and control methods for atomic force microscopy in real-time," in *Proceedings of the American Control Conference*, 2007, pp. 3503–3508.

[9] M. Anwar and I. Rousso, "Atomic force microscopy with time resolution of microseconds," *Applied Physics Letters*, vol. 86, no. 1, p. 014101, January 2005.

[10] G. Schitter and A. Stemmer, "Identification and open-loop tracking control of a piezoelectric tube scanner for high-speed scanning-probe microscopy," *IEEE Transactions on Control Systems Technology*, vol. 12, no. 3, pp. 449–454, May 2004.

[11] S. M. Salapaka, A. Sebastian, J. P. Cleveland, and M. V. Salapaka, "High bandwidth nano-positioner: A robust control approach," *Review of Scientific Instruments*, vol. 73, no. 9, pp. 3232–3241, September 2002.

[12] Y. Wu and Q. Zou, "Iterative control approach to compensate for both the hysteresis and the dynamics effects of piezo actuators," *IEEE Transactions on Control Systems Technology*, vol. 15, no. 5, pp. 936–944, September 2007.

[13] L. Y. Pao, J. A. Butterworth, and D. Y. Abramovitch, "Combined feedforward/feedback control of atomic force microscopes," in *Proceedings of the American Control Conference*, 2007, pp. 3509–3515.

[14] S. Devsia, E. Eleftheriou, and S. O. R. Moheimani, "A survey of control issues in nanopositioning," *IEEE Transactions on Control Systems Technology*, vol. 15, no. 5, pp. 802–823, September 2007.

[15] S. B. Andersson and D. Y. Abramovitch, "A survey of non-raster scan methods with application to atomic force microscopy," in *Proceedings of the American Control Conference*, 2007, pp. 3516–3521.

[16] S. B. Andersson, "Curve tracking for rapid imaging in AFM," *IEEE Transactions on Nanobioscience*, vol. 6, no. 4, pp. 354–361, 2007.

[17] A. Pressley, *Elementary Differential Geometry*. London, UK: Springer, 2005.

[18] S. B. Andersson and J. Park, "Tip-steering for fast imaging in AFM," in *Proceedings of the American Control Conference*, 2005, pp. 2469–2474.

[19] D. R. Sahoo, A. Sebastian, and M. V. Salapaka, "Transient-signal based sample-detection in atomic force microscopy," *Physical Review Letters*, vol. 83, no. 26, pp. 5521–5523, December 2003.

[20] E. Calabi, P. J. Olver, C. Shakiban, A. Tannenbaum, and S. Haker, "Differential and numerically invariant signature curves applied to object recognition," *International Journal of Computer Vision*, vol. 26, no. 2, pp. 107–135, February 1998.

[21] G. K. Binnig and D. Smith, "Single-tube three dimensional scanner for scanning tunneling microscopy," *Review of Scientific Instruments*, vol. 58, pp. 1688–1689, 1986.